A Regge quark model for $O^{-}1/2^{+} \rightarrow O^{-}1/2^{+}$ scattering

1971 J. Phys. A: Gen. Phys. 4 244

(http://iopscience.iop.org/0022-3689/4/2/010)

J. Phys. A: Gen. Phys., 1971, Vol. 4. Printed in Great Britain

A Regge quark model for $O^-\frac{1}{2}^+ \to O^-\frac{1}{2}^+$ scattering

R. W. MOORE, K. J. M. MORIARTY† and J. H. R. MIGNERON
Physics Department, Imperial College, London SW7, England
MS. received 6th May 1970, *in revised form 5th August* 1970

Abstract. We present results of a Regge quark model fit to 2 body charge exchange and elastic $O^-\frac{1}{2}^+ \to O^-\frac{1}{2}^+$ scattering. Both constant and exponential t-dependent residues are used; the latter giving the better description of the data.

1. Introduction

Previous authors have shown that high-energy 2body meson–baryon scattering data in the peripheral region ($0 \geqslant t \geqslant -1$ (GeV/c)^2) can be fitted by the exchange of a few Regge poles in the t channel. In the following paper, we use a quark model to relate the vertices involved in different processes without using (quark) symmetry breaking, and this provides significant constraints on the parameters. Following Högaasen and Fischer (1966) and also Rarita and Schwarzschild (1967), a ρ' is introduced to get nonzero polarization in $\pi^- p \to \pi^0 n$, but unlike the last quoted authors we find the ρ' plays a significant role in the differential cross sections.

Differential cross sections of $K^+ n$ charge exchange at 2·3 and 3 GeV/c and polarizations of $K^- p$ elastic scattering between 2·0 and 2·4 GeV/c are dealt with. These are the highest energies available for the above data and appear to be free of s channel resonances.

The general Regge formalism is developed in §§ 2 and 3, while in §§ 4 and 5 the quark model features are given. A deuteron correction for $K^+ n$ charge exchange data is given in § 6 and in § 7 a superconvergent sum rule to relate the parameters of the ρ and ρ' is shown. §§ 8 and 9 give respectively the parameterization of the Regge residues and the discussion of our results.

2. General formalism

In analysing $O^-\frac{1}{2}^+ \to O^-\frac{1}{2}^+$ scattering processes we exchange tchannel Regge poles which are treated, for the time being, as physical particles to get the signs of the amplitudes. Thus, isotopic spin considerations allow us to have $I = 0$ or 1 tchannel exchange for elastic scattering but only $I = 1$ exchange for charge exchange scattering. We normalize on $\pi^- p \to \pi^- p$ for pion processes and $K^- p \to K^- p$ for kaon ones for the amplitude signs, giving for both the flip and nonflip amplitudes:

$$A(\pi^- p \to \pi^- p) = A_p^\pi + A_{p'}^\pi + A_{\rho^0}^\pi + A_{\rho'^0}^\pi \tag{2.1a}$$

$$A(\pi^+ p \to \pi^+ p) = A_p^\pi + A_{p'}^\pi - A_{\rho^0}^\pi - A_{\rho'^0}^\pi \tag{2.1b}$$

$$A(K^- p \to K^- p) = A_p^K + A_{p'}^K + A_\omega^K + A_{\rho^0}^K + A_{\rho'^0}^K + A_{A_2^0}^K \tag{2.1c}$$

$$A(K^+ p \to K^+ p) = A_p^K + A_{p'}^K - A_\omega^K - A_{\rho^0}^K - A_{\rho'^0}^K + A_{A_2^0}^K \tag{2.1d}$$

† Science Research Council Fellow.

$$A(K^-n \to K^-n) = A_p^K + A_{p'}^K + A_\omega^K - A_{\rho^0}^K - A_{\rho'^0}^K - A_{A_2^0}^K \tag{2.1e}$$

$$A(K^+n \to K^+n) = A_p^K + A_{p'}^K - A_\omega^K + A_{\rho^0}^K + A_{\rho'^0}^K - A_{A_2^0}^K \tag{2.1f}$$

where the amplitude signs of (2.1*a*) to (2.1*b*), (2.1*c*) to (2.1*d*) and (2.1*e*) to (2.1*f*) are related by the charge conjugation invariance of the 3 meson vertex while those of (2.1*c*) to (2.1*e*) and (2.1*d*) to (2.1*f*) are determined by the SU(2) invariance of the baryon vertex. In (2.1) the ρ' pole is introduced in the charge exchange amplitudes to get nonzero polarization in $\pi^-p \to \pi^0n$. By SU(2) symmetry it then appears also in the elastic amplitudes. By using SU(2) to determine the signs and the quark model to determine the magnitudes, the charge exchange amplitudes are:

$$\begin{aligned}
A(\pi^-p \to \pi^0n) &= A_{\rho^+}^\pi + A_{\rho'^+}^\pi \\
A(\pi^-p \to \eta^0n) &= A_{A_2^+}^\pi \\
A(K^-p \to \bar{K}^0n) &= A_{\rho^+}^K + A_{\rho'^+}^K + A_{A_2^+}^K \\
A(K^+n \to K^0p) &= -A_{\rho^-}^K - A_{\rho'^-}^K + A_{A_2^-}^K .
\end{aligned} \tag{2.2}$$

For pair-wise equal mass $O^-\frac{1}{2}^+ \to O^-\frac{1}{2}^+$ scattering the relevant quantities are the differential cross section $d\sigma/dt$, the polarization P and the total cross section σ_T, as given by:

$$\begin{aligned}
\frac{d\sigma}{dt}(s,t) &= \frac{1}{\pi}\left(\frac{1}{4p}\right)^2\left\{\left(1-\frac{t}{4m^2}\right)|A|^2 - \frac{t}{4m^2}\left(\frac{s+p^2}{1-t/4m^2} - s\right)|B|^2\right\} \\
P\frac{d\sigma}{dt}(s,t) &= \frac{1}{\pi}\left(\frac{1}{8p^2}\right)\left(1-\frac{t}{4m^2}\right)^{1/2}\left\{\left(\frac{s+p^2}{1-t/4m^2} - s\right)\left(-\frac{t}{4m^2}\right)\right\}^{1/2} \\
&\quad \times \{\mathrm{Re}(A)\mathrm{Im}(B) - \mathrm{Re}(B)\mathrm{Im}(A)\} \\
\sigma_T(s) &= \frac{1}{p}[\mathrm{Im}\{A^{el}(s, t=0)\}]
\end{aligned} \tag{2.3}$$

where s is the invariant square of the energy, t the invariant square of momentum transfer, p the incident meson's laboratory momentum, m the target baryon's mass, $A = A' + \{(E + t/4m)B\}/(1 - t/4m^2)$ where A' and B (B same as in 2·3) are the M-function invariant amplitudes and E is the incident meson's laboratory energy.

3. Regge formalism

The amplitudes for the exchange of a t channel Regge pole, i, may be written as (following Rarita and Schwarzschild 1967)

$$\begin{aligned}
A_i &= -a_i(t)\left(-\frac{|\boldsymbol{q}||\boldsymbol{q}'|}{mE_0}\right)^{\alpha_i(t)}\{\alpha_i(t)+\tfrac{1}{2}\}L_{\alpha_i}(w)\left(\frac{\exp\{-i\pi\alpha_i(t)\}\pm 1}{\sin\pi\alpha_i(t)}\right) \\
B_i &= -b_i(t)\left(-\frac{|\boldsymbol{q}||\boldsymbol{q}'|}{mE_0}\right)^{\alpha_i(t)-1}\{\alpha_i(t)+\tfrac{1}{2}\}\frac{d}{dw}L_{\alpha_i(t)}(w)\left(\frac{\exp\{-i\pi\alpha_i(t)\}\pm 1}{\sin\pi\alpha_i(t)}\right)
\end{aligned} \tag{3.1}$$

where $\alpha_i(t)$ is the trajectory function, m the target baryon mass, E_0 a scaling factor, $\boldsymbol{q}, \boldsymbol{q}'$ are the centre of mass t channel 3 momenta of the baryon and meson respectively, $w = -\cos\theta_t$ where θ_t is the t channel scattering angle, $a_i(t)$, $b_i(t)$ are the Regge residues and $+(-)$ refers to even (odd) signature.

In (3.1), the quantity

$$\left(\frac{-|q||q'|}{mE_0}\right) = \left(\frac{(4m^2-t)^{1/2}(4m'^2-t)^{1/2}}{4mE_0}\right) \tag{3.2}$$

(where m' is the meson mass) is factored out of the residues to cancel the anomalous t channel threshold singularities in the amplitudes due to the appearance of w in the high energy limit of $L_{\alpha_i(t)}(w)$.

$L_{\alpha_i(t)}(w)$ is defined as

$$\begin{aligned} &\alpha_i(t) \geqslant 0 \quad : \quad P_{\alpha_i(t)}(w) \\ &\alpha_i(t) < 0 \quad : \quad -\frac{\tan \pi\alpha_i(t)}{\pi} Q_{-\alpha_i(t)-1}(w) \\ &\xrightarrow[\text{in the high energy limit}]{} \frac{(2w)^{\alpha_i(t)}}{\sqrt{\pi}} \frac{\Gamma\{\alpha_i(t)+\frac{1}{2}\}}{\Gamma\{\alpha_i(t)+1\}}. \end{aligned} \tag{3.3}$$

Also,

$$\frac{\mathrm{d}}{\mathrm{d}w} L_{\alpha_i(t)}(w) = \frac{\alpha_i(t)\{wL_{\alpha_i(t)}(w) - L_{\alpha_i(t)-1}(w)\}}{w^2-1}. \tag{3.4}$$

Hence, (3.1) in the high energy limit becomes

$$\begin{aligned} A_i &= -a_i(t)\left(\frac{2E}{E_0}\right)^{\alpha_i(t)} \frac{\{\alpha_i(t)+\frac{1}{2}\}}{\sqrt{\pi}} \frac{\Gamma\{\alpha_i(t)+\frac{1}{2}\}}{\Gamma\{\alpha_i(t)+1\}} \left(\frac{\exp\{-i\pi\alpha_i(t)\}\pm 1}{\sin \pi\alpha_i(t)}\right) \\ B_i &= -b_i(t)\left(\frac{2E}{E_0}\right)^{\alpha_i(t)-1} \frac{2\alpha_i(t)\{\alpha_i(t)+\frac{1}{2}\}}{\sqrt{\pi}} \frac{\Gamma\{\alpha_i(t)+\frac{1}{2}\}}{\Gamma\{\alpha_i(t)+1\}} \\ &\quad \times \left(\frac{\exp[-i\pi\{\alpha_i(t)\}]\pm 1}{\sin \pi\alpha_i(t)}\right). \end{aligned} \tag{3.5}$$

In this limit, as no $\alpha_i(t)$ reaches -2 for all i,

$$\frac{\Gamma\{\alpha_i(t)+\frac{1}{2}\}}{\Gamma\{\alpha_i(t)+1\}}$$

is replaced by

$$\frac{\alpha_i(t)+1}{\alpha_i(t)+\frac{1}{2}}$$

as a method of removing unwanted poles at $\alpha_i(t) = -1$ and zeros of $\alpha_i(t) = -\frac{1}{2}$.

Thus our amplitudes in the high energy limit are†

$$\begin{aligned} A_i &= -C_i(t)\{\alpha_i(t)+1\}\left(\frac{\exp\{-i\pi\alpha_i(t)\}\pm 1}{\sin \pi\alpha_i(t)}\right)\left(\frac{E}{E_0}\right)^{\alpha_i(t)} \\ B_i &= -D_i(t)\alpha_i(t)\{\alpha_i(t)+1\}\left(\frac{\exp\{-i\pi\alpha_i(t)\}\pm 1}{\sin \pi\alpha_i(t)}\right)\left(\frac{E}{E_0}\right)^{\alpha_i(t)-1} \end{aligned} \tag{3.6}$$

(3.6) suffices for odd signature trajectories, but for even signature ones the 'Chew

† It will be noticed that the formalism brings in the $\{\alpha_i(t)\}^{\frac{1}{2}}$ contributed to the flip amplitude by the nonsense baryon vertex plus the $\{\alpha_i(t)\}^{1/2}$ extracted from the residue to prevent a branch point at $\alpha_i(t) = 0$.

ghost-killing mechanism' is used to remove poles at $\alpha_i(t) = 0$, so in (3.6) we get

$$A_i \to \alpha_i(t) A_i$$
$$B_i \to \alpha_i(t) B_i. \tag{3.7}$$

However, for the low energy K^+n charge exchange scattering, the exact Legendre form of the amplitudes are used, giving, on comparison of (3.6) and (3.5),

$$A_i = -C_i(t)\{\alpha_i(t)+1\}\frac{\Gamma\{\alpha_i(t)+1\}}{\Gamma\{\alpha_i(t)+\frac{1}{2}\}}\frac{\sqrt{\pi}}{2^{\alpha_i(t)}}\left(-\frac{|q||q'|}{mE_0}\right)^{\alpha_i(t)} L_{\alpha_i(t)}(w)\left(\frac{\exp\{-i\pi\alpha_i(t)\}\pm 1)}{\sin\pi\alpha_i(t)}\right)$$

$$B_i = -D_i(t)\{\alpha_i(t)+1\}\frac{\Gamma\{\alpha_i(t)+1\}}{\Gamma\{\alpha_i(t)+\frac{1}{2}\}}\frac{\sqrt{\pi}}{2^{\alpha_i(t)}}\left(-\frac{|q||q'|}{mE_0}\right)^{\alpha_i(t)-1}\frac{\mathrm{d}}{\mathrm{d}w}$$
$$\times L_{\alpha_i(t)}(w)\left(\frac{\exp\{-i\pi\alpha_i(t)\}\pm 1}{\sin\pi\alpha_i(t)}\right). \tag{3.8}$$

We consider scattering only in the peripheral region, so we parameterize our trajectories by the linear approximation:

$$\alpha_i(t) = \alpha_i{}^0 + \alpha_i{}'t. \tag{3.9}$$

4. Quark model predictions

By treating the Regge poles as physical particles, the quark decomposition for the external particles and Regge poles is obtained as in table 1. With this decomposition, we make the following assumptions for the quark model of the scattering:

Table 1. Quark decomposition for external particles and Regge poles treated as physical particles

Particle	Quark structure	J^P
π^+	$p\bar{n}$	
π^-	$n\bar{p}$	
π^0	$\frac{1}{\sqrt{2}}(p\bar{p}-\bar{n}n)$	
K^+	$p\bar{\Lambda}$	0^-
K^-	$\Lambda\bar{p}$	
K^0	$n\bar{\Lambda}$	
$\bar{K}^0$	$\bar{n}\Lambda$	
η^0	$\frac{0{\cdot}86}{\sqrt{2}}(p\bar{p}+n\bar{n})-0{\cdot}52\Lambda\bar{\Lambda}$	
ϕ	$\Lambda\bar{\Lambda}$	
	$\frac{1}{\sqrt{2}}(p\bar{p}+n\bar{n})$	
ρ^+	$p\bar{n}$	1^-
ρ^-	$n\bar{p}$	
ρ^0	$\frac{1}{\sqrt{2}}(p\bar{p}-n\bar{n})$	
f_0'	$\Lambda\bar{\Lambda}$	
f_0	$\frac{1}{\sqrt{2}}(pp+n\bar{n})$	
A_2^+	$p\bar{n}$	2^+
A_2^-	n	
A_2^0	$\frac{1}{\sqrt{2}}(p\bar{p}-n\bar{n})$	

(i) Only strange quarks interact with strange ones, and non-strange ones with non-strange ones. This explains why the ϕ and f_0' Regge poles do not contribute as they consist only of strange quarks which cannot couple to nucleons.

(ii) p and n quarks react with the same 'strength', but the Λ quarks have a different reaction 'strength'.

(iii) The ρ' triplet has the same quark decomposition as the ρ one, although it cannot be put in any SU(3) multiplet.

(iv) The P′ can be identified with the f_0.

(v) The Pomeron P has no particular quark structure and so can interact with both strange and non-strange quarks.

(vi) The Regge residues factorize such that in our pole graphs $B(t) = \gamma_{\text{vertex1}}(t)\,\gamma_{\text{vertex2}}(t)$ where $B(t)$ is either $C(t)$ or $D(t)$ in the formalism.

(vii) Quark additivity.

The quark structures of the η^0, ω, ϕ, f_0 and f_0' are determined by mixing.

For the η^0, mixing is assumed between the η_8^0 and η_1^0 where the subscripts denote SU(3) multiplets. Thus

$$\eta^0 = \eta_8^0 \cos\theta - \eta_1^0 \sin\theta \tag{4.1}$$

and by using the normal quark decomposition for η_8^0 and η_1^0, together with the linear form of the Gell-Mann Okubo mass relations, the mixing angle is $-23°$. Similarly, Folk model mixing is assumed for $\omega_8 - \phi_1$, and $f_{08} - f_{01}'$ mixing. Thus we get the quark decomposition of η^0, ω, ϕ, f_0, f'_0 as in table 1.

Relations, independent of momentum transfer, between Regge residues are determined by two methods.

(1) For a given Regge pole, relations for the residues in different reactions with a common vertex are obtained by considering the quark content of external particles only.

(2) For Regge poles in the same SU(3) multiplet (as corresponding multiplets have a similar quark structure), relations are obtained by letting the Regge pole have the same quark structure as the physical particle of the same name.

Methods 1 and 2 are illustrated by the following examples.

For method 1, the ρ^0 Regge pole is considered in the two processes $\pi^-\mathrm{p} \to \pi^-\mathrm{p}$ and $\mathrm{K}^-\mathrm{p} \to \mathrm{K}^-\mathrm{p}$. Assuming factorization,

$$B^{\pi}_{\rho^0}(t) = \gamma_{\pi-\pi-\rho^0}(t)\gamma_{pp\rho^0}(t)$$

$$B^{\mathrm{K}}_{\rho^0}(t) = \gamma_{\mathrm{K}-\mathrm{K}-\rho^0}(t)\gamma_{pp\rho^0}(t)$$

Hence

$$\frac{B^{\pi}_{\rho^0}(t)}{B^{\mathrm{K}}_{\rho^0}(t)} = \frac{\gamma_{\pi-\pi-\rho^0}(t)}{\gamma_{\mathrm{K}-\mathrm{K}-\rho^0}(t)}.$$

To determine this, reference is made to figure 1 and quark additivity is applied. As two quarks interact in $\gamma_{\pi-\pi-}(t)$ (figure 1(*a*)) and only one in $\gamma_{\mathrm{K}-\mathrm{K}-\rho^0}(t)$ (figure 1(*b*)):

$$\frac{B^{\pi}_{\rho^0}(t)}{B^{\mathrm{K}}_{\rho^0}(t)} = 2. \tag{4.2}$$

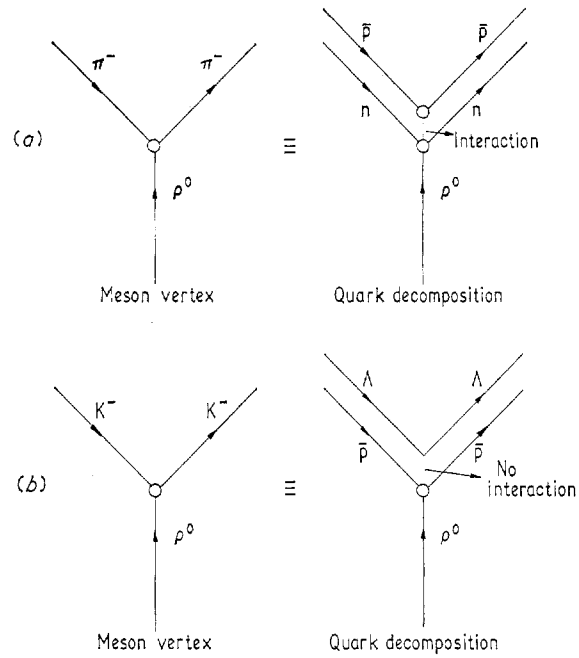

Figure 1. Pole diagram illustrating derivation of quark model relations without assuming specific quark structure for the Regge pole. (In the following figures full lines refer to constant residues and broken lines refer to exponential residues.)

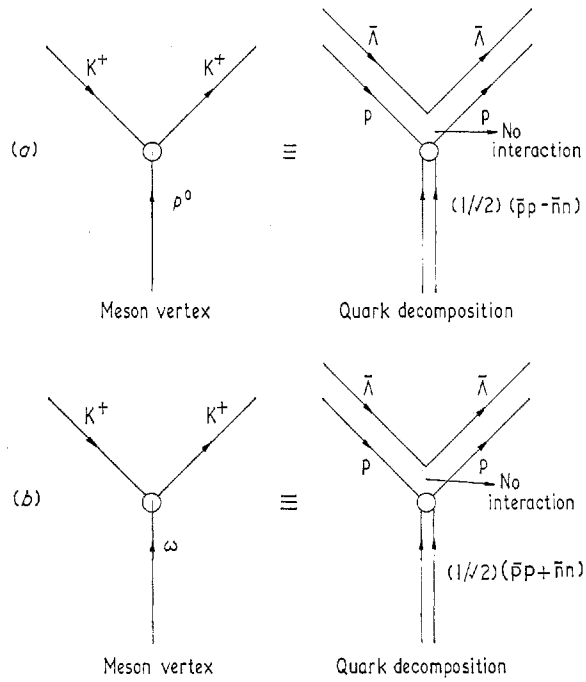

Figure 2. Diagram illustrating derivation of further quark model relations by assuming specific quark structure for the Regge pole.

Similarly, for method 2, the ρ^0 and ω Regge poles are considered at the K^+K^+ Regge pole vertex of $K^+p \to K^+p$. For the ρ^0, the p quark line of K^+ couples with a factor of $1/\sqrt{2}$ and the $\bar{\Lambda}$ quark line of K^+ couples with a factor of $1/\sqrt{2}$. For the ω, the p quark line couples with a factor of $1/\sqrt{2}$ and again the $\bar{\Lambda}$ has no coupling. Hence (see figure 2).

$$\gamma_{K^+K^+\rho^0}(t) = \gamma_{K^+K^+\omega}(t). \tag{4.3}$$

These two methods combine to give the relations in table 2, where we have eight independent residues (Four $C_i(t)$ and four $D_i(t)$, both specified by the B); two each for 1^- and 2^+ SU(3) multiplets plus two each for the ρ' and the Pomeron.

Table 2. Quark model constraints on the Regge residues where *B* can be both nonflip or flip residue

Independent residues	Constraints
	$B^K_{\rho^\pm} = 2B^\pi_{\rho^0}$
$B^\pi_{\rho^0}$	$B^\pi_{\rho^\pm} = 2\sqrt{2}B^\pi_{\rho^0}$
	$B^K_{\rho^0} = \frac{1}{2}B^\pi_{\rho^0}$
	$B^K_\omega = \frac{3}{2}B^\pi_{\rho^0}$
	$B^K_{\rho'^\pm} = 2B^\pi_{\rho'^0}$
$B^\pi_{\rho'^0}$	$B^\pi_{\rho'^\pm} = 2\sqrt{2}B^\pi_{\rho^0}$
	$B^K_{\rho'^0} = \frac{1}{2}B^\pi_{\rho'^0}$
	$B^\pi_{A_2^\pm} = \frac{3}{2}B^{K^\pm}_A$
$B^{K^\pm}_{A_2}$	$B^K_{A_2^0} = \frac{1}{4}B^{K^\pm}_{A_2}$
	$B^K_{p'} = \frac{3}{4}B^{K^\pm}_{A_2}$
	$B^\pi_{p'} = \frac{3}{2}B^{K^\pm}_{A_2}$
B^K_p	$B^\pi_p = \dfrac{2}{1+\gamma_{q_\Lambda q_\Lambda p}/\gamma_{q_N q_N p}} B^K_p$

5. Scaling factor E_0 in the quark model

As shown by James and Watson, quark model amplitudes should be compared at equal values of the relative velocity of the incident meson to the target baryon in the laboratory frame. Thus, by choosing E_0 to be the mass of the incident meson, $E/E_0 = 1/(1-v^2)^{1/2}$ where v is the required relative velocity and so the above condition is satisfied. This, however, only applies to pair-wise equal mass scattering, so in the case of $\pi^- p \to \eta^0 n$, we choose E_0 to be $(m_\pi m_\eta)^{1/2}$.

6. Deuteron correction in $K^+n \to K^0p$

The data for this reaction is obtained from $K^+d \to K^0pp$ where one proton remains a 'spectator'. Hence the experimental result is $(d\sigma/dt)_d$ whereas the theoretical

prediction is $(d\sigma/dt)_n$. A correction to the theoretical result is given by

$$\left(\frac{d\sigma}{dt}\right)_d = \left(\frac{d\sigma}{dt}\right)_n \left(\frac{1-H+R(1-\frac{1}{3}H)}{1+R}\right) \tag{6.1}$$

where

$$R(t) = \frac{(d\sigma/dt)_n\,(\text{flip component})}{(d\sigma/dt)_n\,(\text{nonflip component})}$$

and

$$H(t) = \int d^3\boldsymbol{r}\,|\psi_d(\boldsymbol{r})|^2 \exp\{i(\boldsymbol{p}'-\boldsymbol{p})\,.\,\boldsymbol{r}\}$$

in which

$$\psi_d(\boldsymbol{r}) = 2\pi\left(\omega+\rho-\frac{4\omega\rho}{\omega+\rho}\right)^{-1/2}\left\{\exp\left(-\frac{\boldsymbol{r}}{\omega}\right)-\exp\left(-\frac{\boldsymbol{r}}{\rho}\right)\right\}$$

the Hulthen deuteron wavefunction with $\rho/\omega \sim \frac{1}{7}$, $\omega \simeq 4{\cdot}31\times10^{-13}$ cm and the momentum of the K^0 is $\boldsymbol{p}'$ for a free neutron target and $\boldsymbol{p}$ for a deuteron one.

7. Igi and Matsuda superconvergent sum rule

This sum rule is used to provide an equation of constraint between $C^{\pi}_{0\rho^0}$, $C^{\pi}_{0\rho'^0}$, α^0_ρ, $\alpha^{0\prime}_{\rho'}$ as shown:

$$4\pi f^2 = \frac{1}{2\pi}\int_{E=m'}^{\infty}\left[p\{\sigma_T(\pi^+p)-\sigma_T(\pi^-p)\}\right.$$
$$\left.-\left\{B^{\pi}_{\rho^0}L_{\alpha^0_\rho}\left(\frac{E}{m'}\right)+B^{\pi}_{\rho'^0}L_{\alpha^0_{\rho'}}\left(\frac{E}{m'}\right)\right\}\right]dE \tag{7.1}$$

where $f^2 = 0{\cdot}081$ is the square of the πN coupling constant, m' is the pion mass and, as $E\to\infty$,

$$\sum_{i=\rho,\rho'} B^{\pi}_i L_{\alpha^0_i}\left(\frac{E}{m'}\right) \to \frac{1}{\sqrt{2}}\,\mathrm{Im}(A_{\pi^-p\to\pi^0n})_{t=0}.$$

Hence

$$B^{\pi}_{\substack{\rho^0\\ \rho'^0}\}} = 2C^{\pi}_{\substack{0\rho^0\\ 0\rho'^0}\}}\left(\alpha^0_{\substack{\rho\\ \rho'}\}}+1\right)\sqrt{\pi}\,\frac{\Gamma(\alpha^0_{\substack{\rho\\ \rho'}\}}+1)}{\Gamma(\alpha^0_{\substack{\rho\\ \rho'}\}}+\frac{1}{2})}\left(\frac{m'}{2E_0}\right)^{\alpha^0_{\substack{\rho\\ \rho'}\}}}. \tag{7.2}$$

We let the upper limit of the integral be about $39m'$ and use Igi's numerical determination of

$$\int_{m'}^{39m'}[p\{\sigma_T(\pi^+p)-\sigma_T(\pi^+p)\}]\,dE\,.$$

8. Parameterization of Regge residues

As quark model relations are independent of momentum transfer, the first attempt to fit the data was made with constant residues. Here there were seven free parameters

$$D^{\pi}_{\rho^0} = D^{\pi}_{0_{\rho^0}},\ D^{\pi}_{\rho'^0} = D^{\pi}_{0\rho'^0},\ C^{K}_{A^{\pm}_2} = C^{K}_{0A^{\pm}_2},\ D^{K}_{A^{\pm}_2} = D^{K}_{0A^{\pm}_2},\ C^{K}_{p} = C^{K}_{0p},\ D^{K}_{p} = D^{K}_{0p}$$

and $C2 = \gamma_{q_\Lambda q_\Lambda p}/\gamma_{q_N q_N p}$ and two parameters related by the superconvergent sum rule that is, $C^{\pi}_{\rho^0} = C^{\pi^0}_{0\rho^0}$ and $C^{\pi}_{\rho'^0} = C^{\pi}_{0\rho'^0}$.

The fits here left much room for improvement so exponential t-dependent residues were introduced, giving 15 free parameters and two ($C_{0\rho}^{\pi\,0}$ and $C_{0\rho'0}$) restricted by the sum rule leading to residues:

$$C_{\rho^0}^{\pi}(t) = C_{0\rho^0}^{\pi} \exp(C_{1\rho^0}^{\pi} t) \qquad D_{\rho^0}^{\pi}(t) = D_{0\rho^0}^{\pi} \exp(D_{1\rho^0}^{\pi} t)$$

$$C_{\rho'^0}^{\pi}(t) = C_{0\rho'^0}^{\pi} \exp(C_{1\rho'^0}^{\pi} t) \qquad D_{\rho'^0}^{\pi}(t) = D_{0\rho'^0}^{\pi} \exp(D_{1\rho'^0}^{\pi} t)$$

$$C_{A_2^{\pm}}^{\mathrm{K}}(t) = C_{0A^{\pm}}^{\mathrm{K}} \exp(C_{1A_2^{\pm}}^{\mathrm{K}} t) \qquad D_{A_2^{\pm}}^{\mathrm{K}}(t) = D_{0A^{\pm}}^{\mathrm{K}} \exp(D_{1A_2^{\pm}}^{\mathrm{K}} t)$$

$$C_p^{\mathrm{K}}(t) = C_{0p}^{\mathrm{K}} \exp(C_{1p}^{\mathrm{K}} t) \qquad D_p^{\mathrm{K}}(t) = D_{0p}^{\mathrm{K}} \exp(D_{1p}^{\mathrm{K}} t)$$

with the 17th parameter $C2 = \gamma_{q_\Delta q_\Delta p}/\gamma_{q_N q_N p}$.

There was only one C_1, and one D_1 to each SU(3) multiplet to avoid breaking the quark model constraints. The exponential t-dependent residues gave an improved fit.

9. Results and discussions

As the Regge trajectories appear to be reasonably consistent between authors, the parameters of the trajectories, $\alpha_i{}^0$ and α_i', were kept fixed as in table 3. The other

Table 3. Parameters for the Regge trajectories

Regge pole	α^0	α' (GeV)$^{-2}$
ρ	0·58	0·92
ρ'	−0·48	1·44
A_2	0·37	0·41
P	1·00	0·12
P'	0·73	1·5
ω	0·45	0·31

parameters, described in § 4, result from an χ^2 fit to the data using the minimizing program MINUIT (CERN Program Library No. D506), and are given in tables 4 and 5. Those in table 4 result from an attempt to fit the data using constant residues with the quark model constraints, relying on the scale factor $(E_0)^{-\alpha_i(t)}$ to give the t-dependence. The χ^2 fits so obtained left considerable room for improvement particularly in the elastic scattering differential cross sections, which are of shape $\exp(-at)$. Thus, we feel that using the scale factor did not give enough freedom to

Table 4. Values of the independent constant residues and associated parameters

Parameter in (mbn GeV)		Parameter in (mbn)	
$C_{0\rho^0}^{\pi}$	0·45	$D_{0\rho^0}^{\pi}$	−66·14
$C_{0\rho'^0}^{\pi}$	12·93	$D_{0\rho'^0}^{\pi}$	−256·28
$C_{0A_2^{\pm}}^{\mathrm{K}}$	−3·23	$D_{0A_2^{\pm}}^{\mathrm{K}}$	−155·79
C_{0}^{K}	−0·54	D_{0p}^{K}	−2·25

$C2 = 3.40$

obtain the required a to fit the data. This was remedied by the introduction of exponential t-dependent residues giving the parameter values as in table 5, but these residues did not improve the charge-exchange scattering, probably because the

Table 5. Parameters describing the exponential t-dependent residues

Parameter in (mbn GeV)		Parameter in $(\text{GeV}/c)^{-2}$		Parameter in (mbn)		Parameter in $(\text{GeV}/c)^{-2}$	
$C_{0\rho^0}^{\pi}$	0·49	$C_{1\rho^0}^{\pi}$	−1·65	$D_{0\rho^0}^{\pi}$	−57·30	$D_{1\rho^0}^{\pi}$	1·12
$C_{0\rho'^0}^{\pi}$	0·57	$C_{1\rho'^0}^{\pi}$	85·50	$D_{0\rho'^0}^{\pi}$	2332·44	$D_{1\rho'^0}^{\pi}$	13·65
$C_{0A_2^{\pm}}^{K}$	−1·41	$C_{1A_2^{\pm}}^{K}$	−0·75	$D_{0A_2^{\pm}}^{K}$	94·24	$D_{1A^{\pm}}^{K}$	−1·24
C_{0p}^{K}	−1·46	C_{1p}^{K}	2·03	D_{0p}^{K}	36·19	D_{1p}^{K}	3·40
			C2 = 2·28				

Table 6. χ^2 for fits to individual data

Process	No. of data points	χ^2 with constant residues	χ^2 with exponential t-dependent residues
$\sigma_T(K^-p) - \sigma_T(K^-n)$	7	91	77
$\sigma_T(K^+p) - \sigma_T(K^+n)$	9	221	24
$\sigma_T(\pi^-p) - \sigma_T(\pi^+p)$	15	4	16
$\frac{d\sigma}{dt}(\pi^-p \to \eta^0 n)$	44	411	592
$\frac{d\sigma}{dt}(\pi^-p \to \pi^0 n)$	73	692	704
$\frac{d\sigma}{dt}(K^-p \to \bar{K}^0 n)$	33	304	49
$\frac{d\sigma}{dt}(K^+n \to K^0 p)$	28	63	185
$\frac{d\sigma}{dt}(\pi^-p \to \pi^-p)$	150	12 569	618
$\frac{d\sigma}{dt}(\pi^+p \to \pi^+p)$	119	6062	475
$\frac{d\sigma}{dt}(K^-p \to K^-p)$	50	1703	235
$\frac{d\sigma}{dt}(K^+p \to K^+p)$	50	1926	275
$P(\pi^-p \to \pi^0 n)$	17	16	96
$P(\pi^-p \to \pi^-p)$	60	1601	820
$P(\pi^+p \to \pi^+p)$	25	91	1008
$P(K^-p \to K^-p)$	32	1919	703
$\frac{\text{Re}A(0)}{\text{Im}A(0)}(\pi^-p \to \pi^-p)$	6	22	6
$\frac{\text{Re}A(0)}{\text{Im}A(0)}(\pi^+p \to \pi^+p)$	3	11	1
Total	721	27 649	5883

minimizing program concentrated on reducing the large χ^2 of the elastic scattering at the expense of the charge exchange. The χ^2 for the various processes are given in table 6.

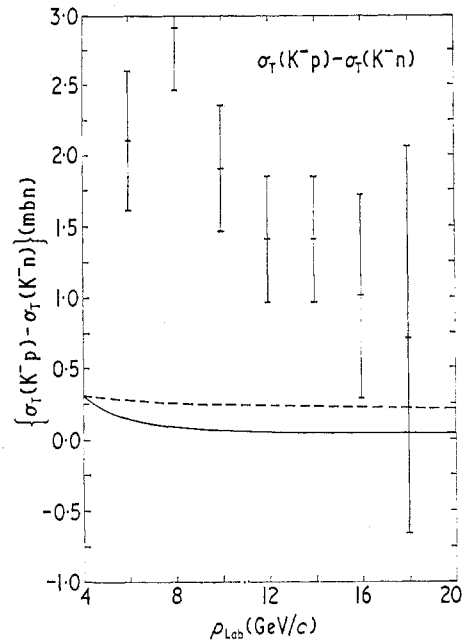

Figure 3. Difference between total cross sections for K^-p and K^-n elastic scattering. Data from Galbraith *et al.* (1965).

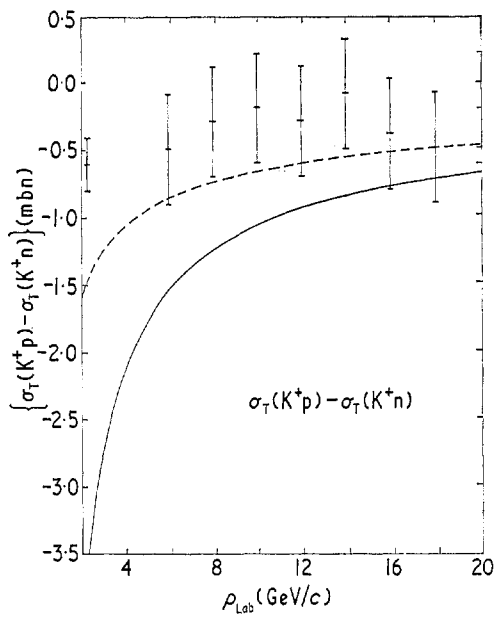

Figure 4. Difference between total cross sections for K^+p and K^+n elastic scattering. Data from Galbraith *et al.* (1965) and Kycia (1967).

These χ^2 fits to the data are not as good as in previous authors, but we have used a simple parameterization heavily constrained by the quark model relations without symmetry breaking. Also, as stated by James and Logan (1967), quark model constraints are valid only to a few per cent. The discussion of the results for each process now follows.

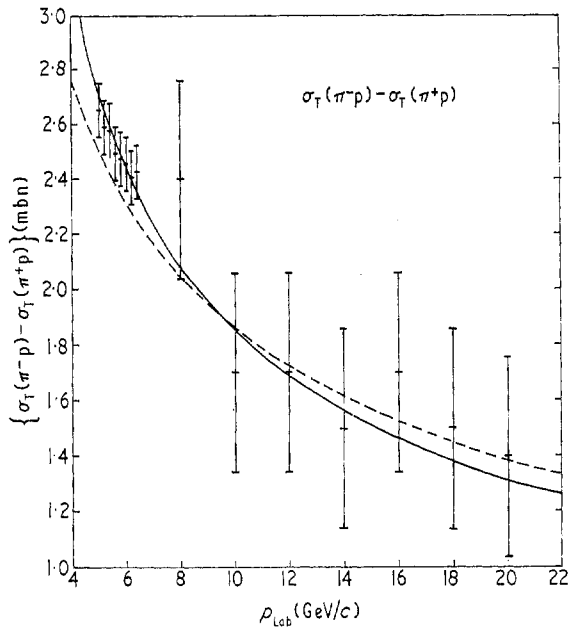

Figure 5. Difference between total cross sections for π^-p and π^+p elastic scattering. Data from Galbraith *et al.* (1965) and Citron *et al.* (1966).

Figures 3, 4 and 5 show total cross-section differences as a function of the meson laboratory momentum. Figure 5 shows $\sigma_T(\pi^-p)-\sigma_T(\pi^+p)$ where ρ and ρ' Regge poles are exchanged. The good χ^2 fit results from the application of the sum rule, giving a curve of shape $E^{-1/2}$ showing ρ' dominance. Thus it is assumed that (except for a quark model factor) these poles would give a similar shape in figures 3 and 4, so the actual shapes in figures 3 and 4 are given by the interference of the A_2 Regge pole with the appropriate sign. This viewpoint is not compatible with the recent Serpukov data in range 30–60 GeV/c (Lund 1969).

Figure 6 shows the differential cross section for $\pi^-p \to \eta^0 n$. As the data here came only from the decay mode $\eta^0 \to 2\gamma$, the theoretical result was multiplied by this branching ratio which was taken as $\frac{1}{3}$, although it has been taken variously as going from 0·3 to 0·38 so a modification here may have improved the fit. The t-dependence was not carried far enough to get the zero predicted by the Chew 'Ghost-killing' mechanism at just beyond $t = -0{\cdot}9$ (GeV/c).

The $\pi^-p \to \pi^0 n$ differential cross section is given in figure 7. The required dip at about $t = -0{\cdot}6$ (GeV/c)^2 is not obtained as the ρ' contribution is no longer small so the predicted dip in the contribution of the ρ at about $t = -0{\cdot}6$ (GeV/c)^2 is smothered.

In figure 8, the $K^-p \to \bar{K}^0 n$ differential cross section is shown. The dip at about $t = -0{\cdot}9$ (GeV/c)^2 in the exponential residue case is probably an A_2 effect.

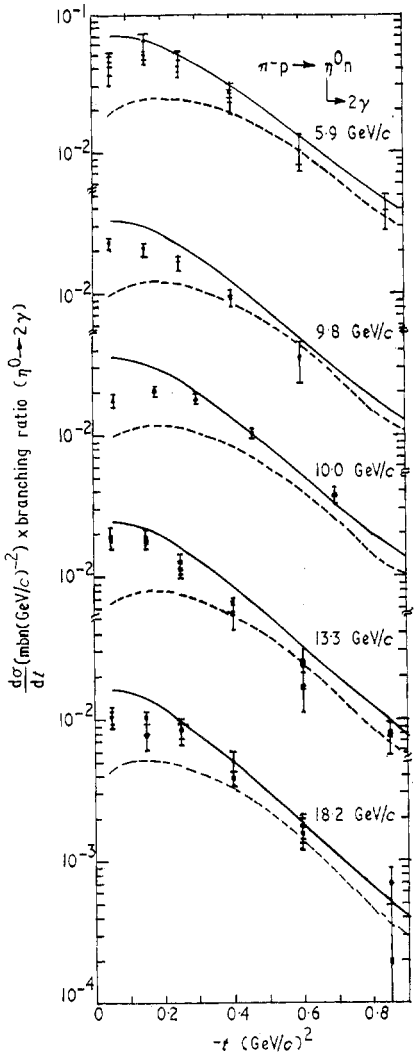

Figure 6. Differential cross sections for $\pi^- p \rightarrow \eta^0 n$. Data from Stirling *et al.* (1965 and 1966) and Wahlig and Mannelli (1968).

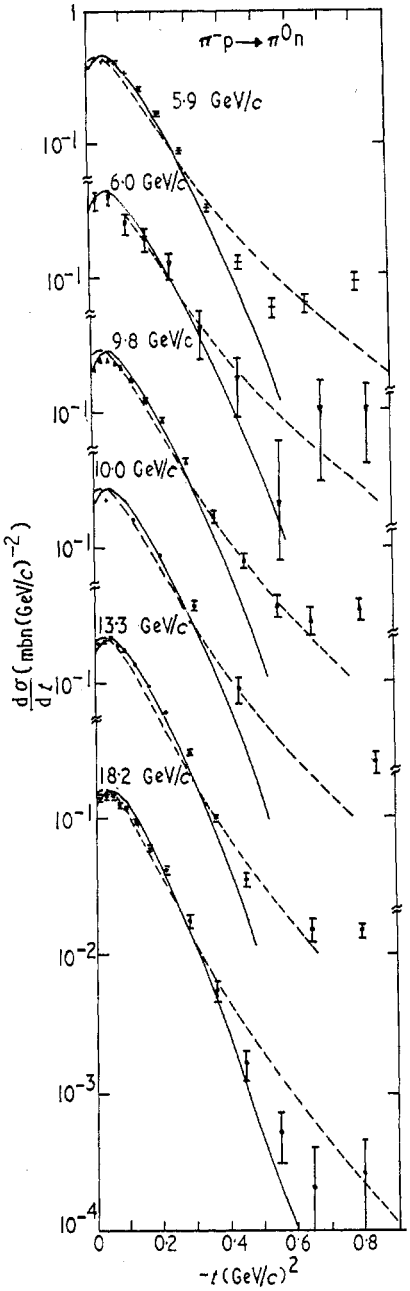

Figure 7. Differential cross sections for $\pi^- p \rightarrow \pi^0 n$. Data from Stirling *et al.* (1965 and 1966) and Wahlig and Mannelli (1968).

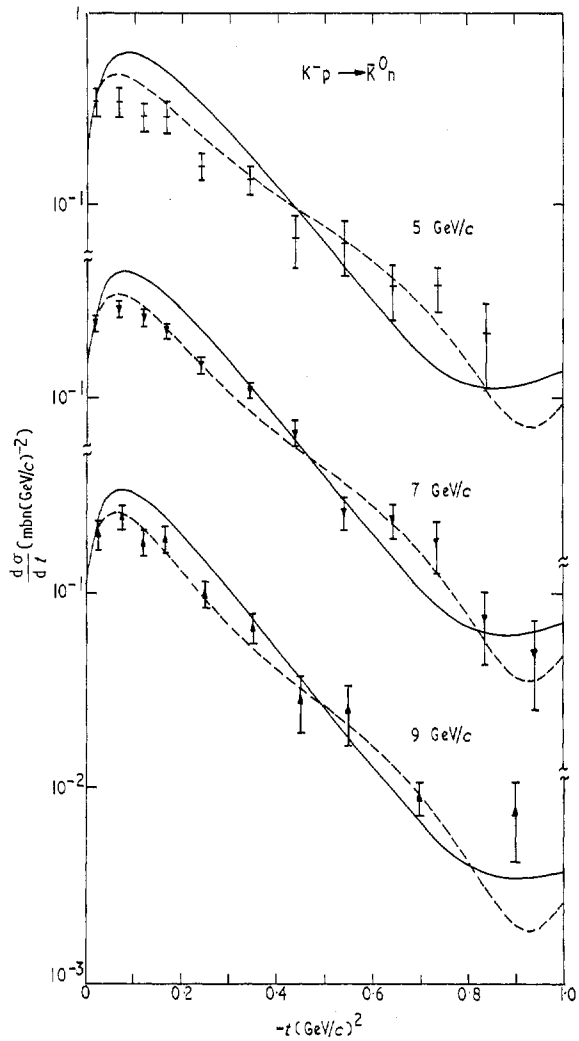

Figure 8. Differential cross sections for $K^-p \to \bar{K}^0n$. Data from Astbury *et al.* (1966).

Figure 9 displays the differential cross section for $K^+n \rightarrow K^0p$. The deuteron correction is found to have the same form as in Rarita and Schwarzschild, but it is found, probably owing to our questionable fit, that the Legendre form is displaced lower than the data although the levelling off at large t, as indicated by the data, is obtained.

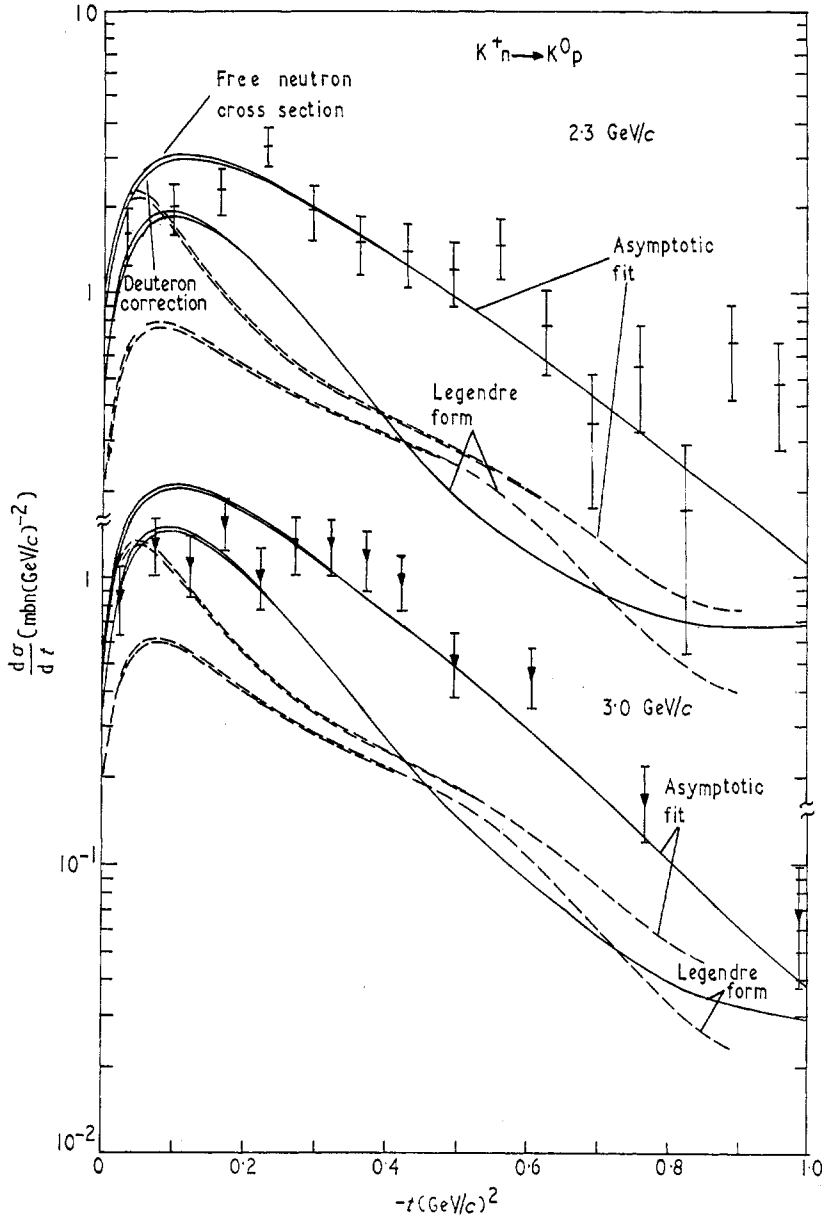

Figure 9. Differential cross sections for $K^+n \rightarrow K^0p$. Data from Butterworth *et al.* (1965) and Goldschmidt-Clermont *et al.* (1968).

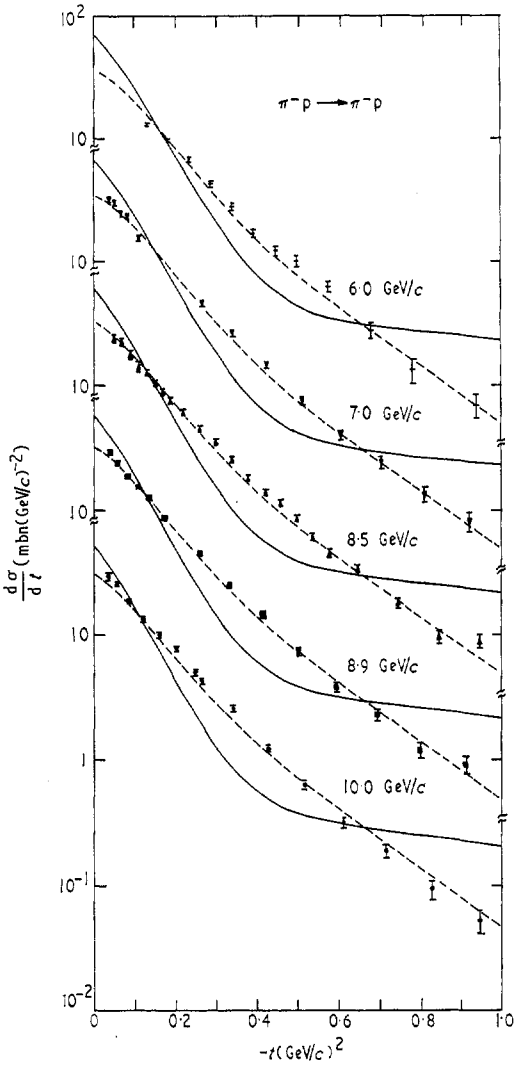

Figure 10. Differential cross sections for $\pi^-p \to \pi^-p$. Data from Foley *et al.* (1963, 1965), Coffin *et al.* (1967) and Harting *et al.* (1965).

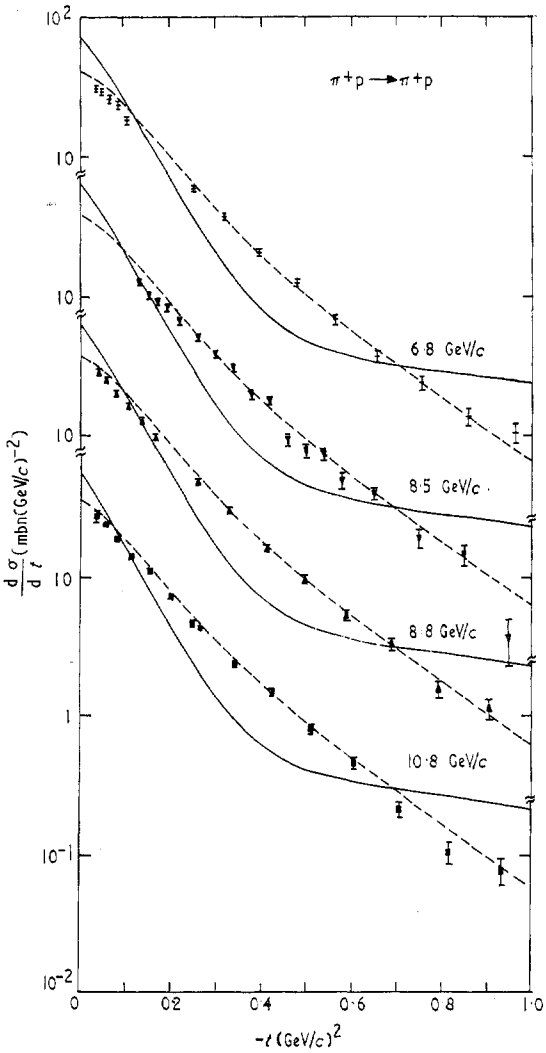

Figure 11. Differential cross sections for $\pi^+p \to \pi^+p$. Data from Foley *et al.* (1963) and Harting *et al.* (1965).

Figures 10 and 11 indicate the differential cross sections for $\pi^{\pm}$p elastic scattering. Here, the improvement using exponential t-dependence residues is dramatic, mainly owing to the shape indicated by the data. Although no crossover effect was obtained, this could have been obtained by extra parameterization.

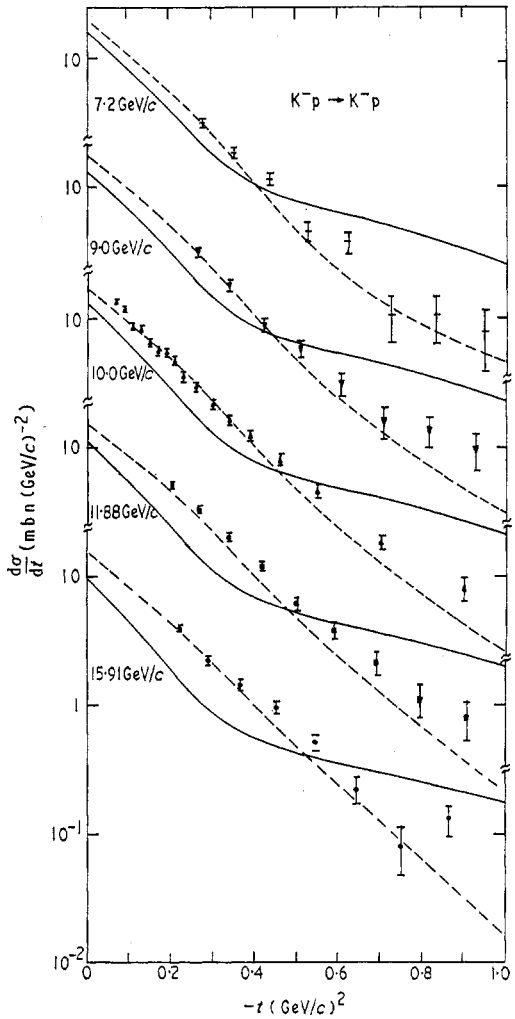

Figure 12. Differential cross sections for $K^-p \rightarrow K^-p$. Data from Foley *et al.* (1965), Harting *et al.* (1965) and Aderholz *et al.* (1967).

Figures 12 and 13 display the differential cross sections for elastic K^-p and K^+p scattering which, as with other curves, exhibited a great improvement with exponential residues. Figure 14 shows the $\pi^-p \rightarrow \pi^0n$ polarization. The noticeable feature here is that constant residues give a better fit than do the exponential ones.

Figures 15 to 18 show the elastic scattering polarization. In figures 15 and 16 the general shape of the two curves appears to be independent of the diagram, leading to the conclusion of P–P' dominance, which, with no change of sign under charge conjugation, leads to a large χ^2 for the exponential residue case. The K^-p elastic

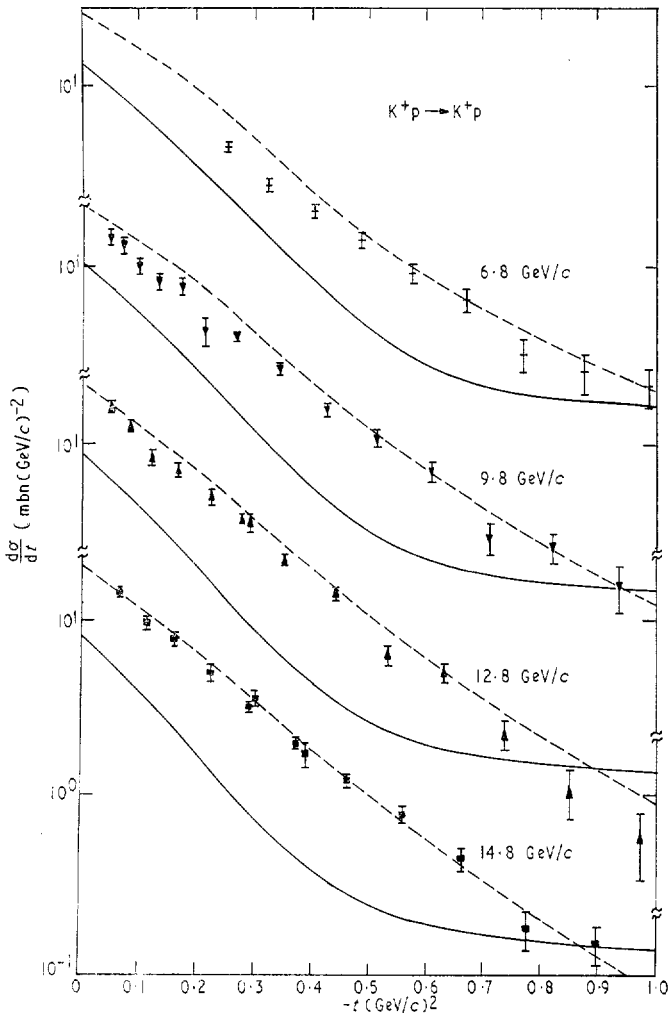

Figure 13. Differential cross sections for $K^+p \to K^+p$. Data from Foley *et al.* (1963).

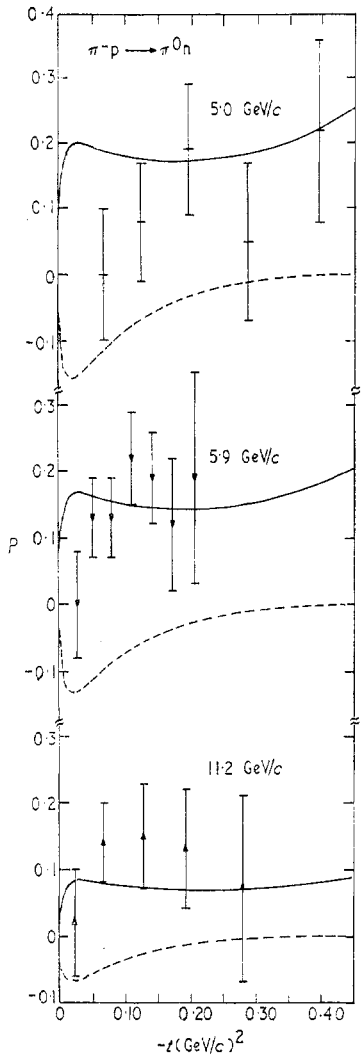

Figure 14. Polarization for $\pi^- p \to \pi^0 n$. Data from Bonamy *et al.* (1966) and Drobnis *et al.* (1968).

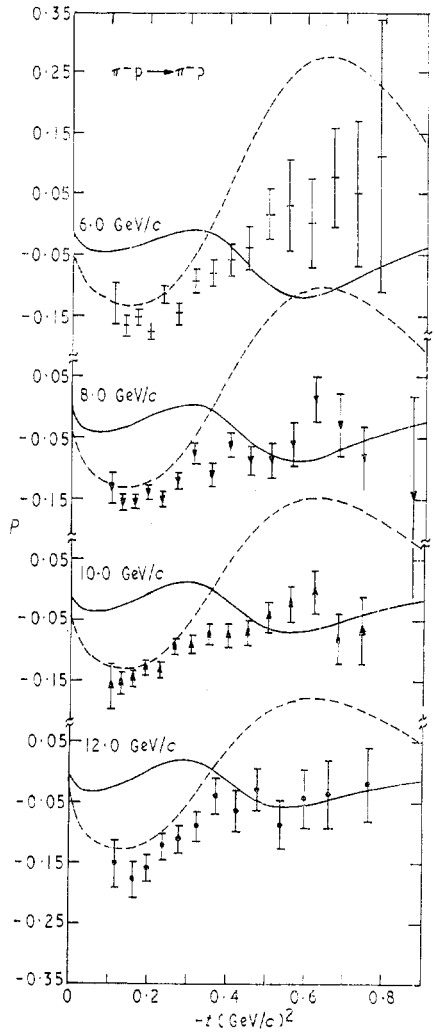

Figure 15. Polarization for $\pi^- p \to \pi^- p$. Data from Borghini *et al.* (1966).

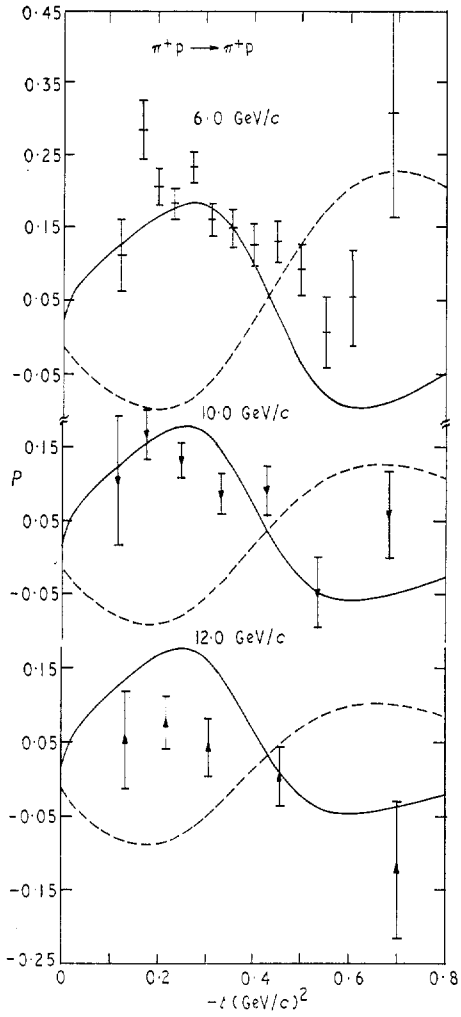

Figure 16. Polarization for $\pi^+p \to \pi^+p$. Data from Borghini *et al.* (1966).

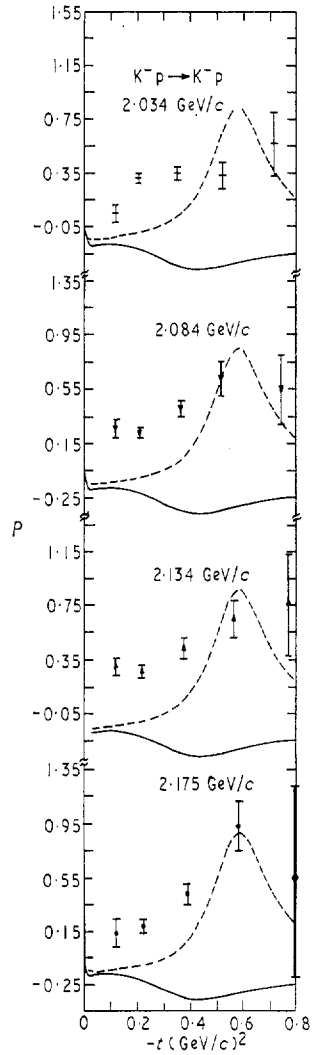

Figure 17. Polarization for $K^-p \to K^-p$. Data from Daum *et al.* (1968).

scattering polarization in figures 17 and 18 follow a similar, although much modified shape, leading to the conclusion that P–P' dominates in all elastic scattering polarization. However, not too much weight can be put on this last set of results owing to the very low energy.

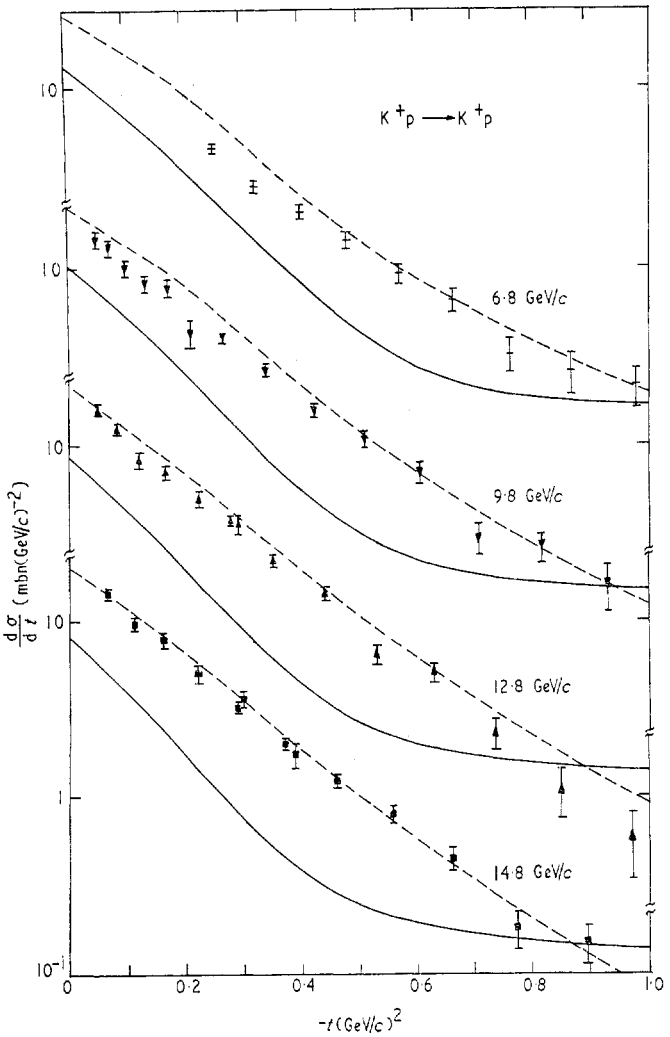

Figure 18. Polarization for $K^-p \to K^-p$. Data from Daum *et al.* (1968).

Although we have not included the diagrams for the ratio of the real part to the imaginary part of the nonflip amplitude in the forward direction for πp elastic scattering, the calculations were carried out, the exponential residues giving the better result.

Thus we feel that a more sophisticated parameterization, together with indicated quark model improvements, could lead to a good χ^2 fit to the data.

Acknowledgments

The authors are indebted to Professor P. T. Matthews for the encouragement and

help in completing this manuscript and also to R. C. Beckwith for assistance with computing. R.W.M. wishes to thank the Science Research Council for a research studentship.

References

ADERHOLZ, M., *et al.* 1967, *Phys. Lett.*, **24B,** 434–7.
ASTBURY, P., *et al.*, 1966, *CERN Rep.*, No. 66/1056/5.
BONAMY, J., *et al.*, 1966, *Phys. Lett.*, **23,** 501–5.
BORGHINI, M., *et al.*, 1966, *Phys. Lett.*, **21,** 114–7.
BUTTERWORTH, I., *et al.*, 1965, *Phys. Rev. Lett.*, **15,** 734–6.
CITRON, A., *et al.* 1966, *Phys. Rev.*, **144,** 1101–4.
COFFIN, C. T., *et al.*, 1967, *Phys. Rev.*, **159,** 1169–75.
DAUM, C., *et al.*, 1968, *Nucl. Phys.*, **B6,** 273–324.
DROBNIS, D. D., *et al.*, 1968, *Phys. Rev. Lett.*, **20,** 274–8.
FOLEY, K. J., *et al.*, 1963, *Phys. Rev. Lett.*, **11,** 425–529, 503–6.
—— 1965, *Phys. Rev. Lett.*, **14,** 862–6, **15,** 45–50.
GALBRAITH, W., *et al.*, 1965, *Phys. Rev.*, **138,** B913–20.
GOLDSCHMIDT-CLERMONT, Y., *et al.*, 1968, *Phys. Lett.*, **27B,** 602–4.
HARTING, D., *et al.*, 1965, *Nuovo Cim.*, **38,** 60–94.
HOGAASON, H., and FISCHER, W., 1966, *Phys. Lett.*, **22,** 516–9.
IGI, K., and MATSUDA, S., 1967, *Phys. Rev. Lett.*, **18,** 625–7.
JAMES, P. B., and LOGAN, R. K., 1967, *Phys. Lett.*, **25B,** 38–40.
JAMES, P. B., and WATSON, H. D. D., 1967, *Phys. Rev. Lett.*, **18,** 179–82.
KYCIA, T., 1967, *Bull. Am. Phys. Soc.*, **12,** 567.
LUND, 1969, 15*th Int. Conf. on Elementary Particles.*
RARITA, W., and SCHWARZSCHILD, B. M., 1967, *Phys. Rev.*, **162,** 1378–85.
STIRLING, A., *et al.*, 1965, *Phys. Lett.*, **18,** 200–3.
—— 1965, *Phys. Rev. Lett.*, **14,** 763–7.
—— 1966, *Phys. Lett.*, **20,** 75–8.
WAHLIG, M. A., and MANNELLI, I., 1968, *Phys. Rev.*, **168,** 1515–26.